2005

Acquisition and Evaluation of Thermodynamic Data for Bieberite-Moorhouseite Equilibria at 0.1 MPa

I-Ming Chou
954 National Center, U.S. Geological Survey, Reston, Virginia 20192, U.S.A., imchou@usgs.gov

Robert Seal II
U.S. Geological Survey, Reston, Virginia 20192, U.S.A.

American Mineralogist, Volume 90, pages 912–917, 2005

Acquisition and evaluation of thermodynamic data for bieberite-moorhouseite equilibria at 0.1 MPa

I-Ming Chou* and Robert R. Seal II

954 National Center, U.S. Geological Survey, Reston, Virginia 20192, U.S.A.

Abstract

Published estimates for the equilibrium relative humidity (RH) at 25 °C for the reaction: bieberite ($CoSO_4 \cdot 7H_2O$) = moorhouseite ($CoSO_4 \cdot 6H_2O$) + H_2O, range from 69.8 to 74.5%. To evaluate these data, the humidity-buffer technique was used to determine equilibrium constants for this reaction between 14 and 43 °C at 0.1 MPa. Reversals along five humidity-buffer curves yield $\ln K = 18.03–6509.43/T$, where K is the equilibrium constant, and T is temperature in K. The derived standard Gibbs free energy of reaction is 9.43 kJ/mol, which agrees well with several previously reported values based on vapor-pressure measurements. It also agrees well with values calculated from the data derived mostly from calorimetric measurements. Previous studies indicated that the temperature of the invariant point for the assemblage bieberite-moorhouseite-aqueous solution-vapor is near 44.7 °C, and our extrapolated data predict 91.1% RH at this temperature; the predicted position for the invariant point is in excellent agreement with those reported previously.

Introduction

Secondary metal-sulfate salts can be important components of the hydrochemical cycles of metals, sulfur, and acidity at active and abandoned mine sites. Sulfate salts of Fe, which form from the oxidative weathering of pyrite or pyrrhotite, typically are the most common at these sites (Jambor et al. 2000). Salts of common base metals such as Cu, Zn, Ni, and Co, which result from the weathering of sulfide minerals of these metals, also can be found locally at these sites. Acid generated from the oxidation of pyrite or pyrrhotite can attack carbonate and silicate minerals in the country rock to contribute Ca, Mg, Mn, and Al, and yield salts of these elements.

Despite the occurrence of Cu-, Zn-, Ni-, and Co-sulfate salts in nature, these metals more commonly occur as solid solutions in more common sulfate salts such as melanterite [$Fe^{2+}SO_4 \cdot 7H_2O$]. Copper and Zn show extensive solid solution in the melanterite structure, both exceeding 50 mol% and both with possible miscibility gaps (Jambor et al. 2000; Peterson 2002). Solid solution of Ni in the melanterite structure approaches 20 mol%, whereas that for Co is complete (Jambor et al. 2000).

Metals present as major or minor constituents in sulfate salts can have significant impacts on aquatic ecosystems because the salts provide a means of storing metals and subsequently releasing them due to the high solubilities of the salts. Uncertainties in the thermodynamic properties of these salts, especially the Gibbs free energy of formation and the enthalpy of formation, severely limit the ability to model the behavior of these salts in natural and laboratory settings. The uncertainties also hinder the ability to model solid-solution effects in these minerals and the aqueous speciation of high ionic strength solutions in these systems. The humidity-buffer technique was developed recently to resolve discrepancies in the location of dehydration reactions at near-ambient conditions (Chou et al. 2002). To date, the technique has been used to investigate dehydration equilibria of end-member system including those of Fe^{2+} sulfates (Chou et al. 2002), Cu sulfates (Chou et al. 2002), Zn sulfates (Chou and Seal 2005), Mg sulfates (Chou and Seal 2003a), and Ni sulfates (Chou and Seal 2003b). This paper extends our understanding to Co sulfates.

Mineralogy of cobalt sulfates

Bieberite is a member of melanterite group, which consists of monoclinic ($P2_1/c$) sulfate heptahydrate minerals of the type $M^{2+}SO_4 \cdot 7H_2O$, where M represents Fe (melanterite), Cu (boothite), Co (bieberite), Mn (mallardite), and (Zn, Cu) (zinc-melanterite). In contrast, the common Mg sulfate heptahydrate, epsomite [$MgSO_4 \cdot 7H_2O$], is orthorhombic and belongs to the epsomite group, wherein morenosite [$NiSO_4 \cdot 7H_2O$] and goslarite [$ZnSO_4 \cdot 7H_2O$] are additional members (Jambor et al. 2000). Bieberite and mallardite are well known as synthetic compounds, and are more common in nature than boothite and Zn-melanterite, which have been found only at a few localities (Jambor et al. 2000). Bieberite forms a complete solid solution with other members of melanterite group, but miscibility gaps exist in synthetic metal-sulfate heptahydrates precipitated at room temperature for the binary systems of bieberite-epsomite, bieberite-goslarite, and bieberite-morenosite (Aslanian et al. 1972; Balarew et al. 1973; Siebke et al. 1983).

Moorhouseite is one of the six members of the hexahydrite group, which are monoclinic ($C2/c$) sulfate minerals of the type $M^{2+}SO_4 \cdot 6H_2O$, where M represents Mg (hexahydrite), Mn (chvaleticeite), Fe (ferrohexahydrite), Ni (nickelhexahydrite), Co (moorhouseite), and Zn (bianchite). The minerals of the group, except hexahydrite, occur sparingly in nature, and mainly as the oxidation products of sulfide deposits. Moorhouseite has been reported from only two localities, and the cation ratios for the type material are Co:Ni:Mn:Cu:Fe:Zn = 55:25:12:5:3:1

* E-mail: imchou@usgs.gov

0003-004X/05/0506–912$05.00/DOI: 10.2138/am.2005.1695

(Jambor and Boyle 1965). Moorhouseite forms complete solid solution with nickelhexahydrite at 61 °C, and a miscibility gap exists at lower temperatures (Rohmer 1939). FeO substitution at about 27 mol% in moorhouseite at 50 °C was reported by Balarew and Karaivanova (1976). Other hydrated cobalt sulfate minerals, including aplowite ($CoSO_4 \cdot 4H_2O$) and cobaltkieserite ($CoSO_4 \cdot H_2O$; approved by IMA 2002), will not be discussed in this study.

Dehydration equilibrium

The stability of bieberite and moorhouseite can be related by the reaction:

$$\underset{\text{bieberite}}{CoSO_4 \cdot 7H_2O_{(s)}} = \underset{\text{moorhouseite}}{CoSO_4 \cdot 6H_2O_{(s)}} + H_2O_{(g)} \quad (1)$$

where (s) and (g) are solid and gas, respectively. Published estimates for the equilibrium relative humidity (RH) at 25 °C range from 69.8 to 74.5% for the reaction. To evaluate these data, the humidity-buffer technique (Polyanskii et al. 1976; Malinin et al. 1977; 1979; Chou et al. 2002) was used in this study to determine equilibrium constants for this reaction between 14 and 43 °C at 0.1 MPa. Reversals were obtained along five humidity-buffer curves. It should be emphasized that Reaction 1 of this study does not involve an aqueous phase. However, as will be presented later, in the presence of an additional aqueous phase at equilibrium at 0.1 MPa, the system becomes invariant with defined equilibrium temperature and humidity.

The standard Gibbs free energy of reaction, ΔG_r°, for Reaction 1 was then derived from the equilibrium constant, K, using the relation:

$$\Delta G_r^\circ = -RT \ln K = -RT \ln (a_{H_2O}) = -RT \ln (f_{H_2O}/0.1)$$
$$= -RT \ln [(f^*_{H_2O}/0.1) \cdot (\%RH)/100], \quad (2)$$

where R is the gas constant (8.31451 J/mol·K); T is absolute temperature; a_{H_2O} is the activity of H_2O; f_{H_2O} is the equilibrium H_2O fugacity (in MPa); and $f^*_{H_2O}$ is the fugacity of pure H_2O (in MPa). The standard states for minerals and H_2O are pure solids and H_2O gas, respectively, at 0.1 MPa and temperature. Preliminary results were presented by Chou and Seal (2003c).

Previous work

Figure 1 summarizes all previous and current data related to the bieberite-moorhouseite equilibria in terms of temperature and relative humidity. Vapor-pressure measurements were made at 0.1 MPa and 25 °C by Wiedemann (1874) and Schumb (1923), at 20 and 25 °C by Diesnis (1935), between 25 and 45.17 °C by Carpenter and Jette (1923), and between 3 and 42.5 °C by Broers and Van Welie (1965). Thermodynamic data for bieberite and moorhouseite derived from calorimetric measurements were evaluated and compiled by Wagman et al. (1982) and DeKock (1982), and the bieberite-moorhouseite phase boundaries based on these data are shown in Figure 1. Heats of solution of solid $CoSO_4$ and several hydrates, including hepta- and hexahydrates, were determined by Goldberg et al. (1966); these data and many others were included in the compilation of DeKock (1982), and will not be discussed in this paper.

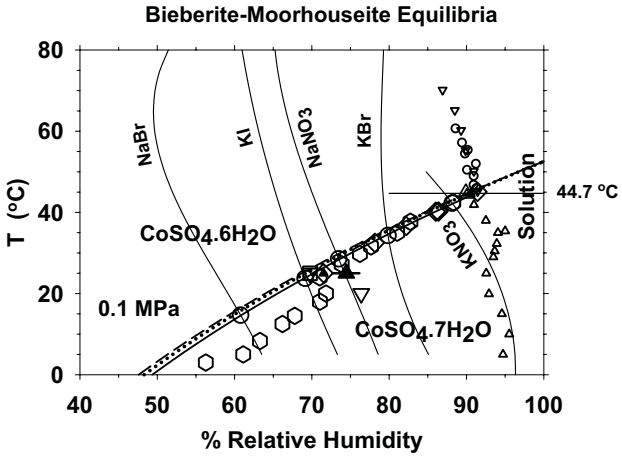

FIGURE 1. Bieberite [$CoSO_4 \cdot 7H_2O$]-moorhouseite [$CoSO_4 \cdot 6H_2O$] equilibria at 0.1 MPa. Results of vapor-pressure measurement at 0.1 MPa and 25 ºC by Wiedemann (1874) and Schumb (1923) are shown by the large solid triangle and the open square, respectively. Also shown are the data of Diesnis (1935) at 20 and 25 °C (open large triangles with the apex pointing down), those between 25 and 45.17 °C reported by Carpenter and Jette (1923; open diamonds), and those between 3 and 42.5 °C reported by Broers and Van Welie (1965; open hexagons). The dashed and dotted lines represent the bieberite-moorhouseite phase boundary based on the thermodynamic data compiled by Wagman et al. (1982) and DeKock (1982), respectively. Experimental results obtained in this study are shown by the large circles along five humidity-buffer cures (near-vertical thin solid lines), and the thick solid line is the least-squares fit for new experimental data. The equilibrium boundary for bieberite-saturated solution is marked by the small open triangles with apexes pointing up (Broers and Van Welie 1965), and by the small solid triangle at 25 ºC and 71.5% RH (Diesnis 1935; this datum is unreliable). The equilibrium boundaries for moorhouseite-saturated solution are marked by the small open triangles with apexes pointing down (Carpenter and Jette 1923), and by the small open circles (Broers and Van Welie 1965). The large open triangle at 44.7 °C (thin solid horizontal line) and 89.9% RH indicates the invariant point for the assemblage bieberite + moorhouseite + aqueous solution + vapor (BMAV) reported by Broers and Van Welie (1965). Our data predict the invariant point at RH = 91.1% at this temperature; for details, see text.

EXPERIMENTAL METHOD AND RESULTS

Starting materials were mixtures of reagent grade $CoSO_4 \cdot 7H_2O$ (GFS Chemicals, Lot no. L608950) and its dehydration product [$CoSO_4 \cdot 6H_2O$]. A weighed amount of the starting material, typically 378 to 567 mg, was loaded into a plastic sample container (8 mm ID x 10 mm OD and 20 mm tall), which was partly immersed in a humidity-buffer solution in a glass container (17.5 mm ID × 20 mm OD and 40 mm tall) sealed by a rubber stopper. Humidity-buffer solutions are saturated solutions with well-characterized humidity variations with temperature (Greenspan 1977; Chou et al. 2002). The present study used five different binary aqueous buffer solutions: NaBr, KI, $NaNO_3$, KBr, and KNO_3 (Fig. 1). The whole assembly was then immersed in a water bath, the temperature of which was controlled to ± 0.03 °C and measured by a Pt resistance probe (accurate to ± 0.02 °C). Small holes through the cap of the sample chamber allow the vapor phase of the sample to equilibrate with that of the buffer system at the fixed temperature for a duration between 46 and 120 hours (Table 1). The direction of reaction was determined by the mass change of the sample (precise to ± 0.05 mg). Results along the KI-saturated buffer solution are shown in Figure 2. Both the starting material and experimental products were examined by X-ray diffraction and optical methods, and no unexpected phases were identified. Uncertainties in predicted%RH for the humidity buffers used in the temperature range of this study are no more than ± 0.11 (Greenspan 1977). Experimental results are listed in Tables 1 and 2, and plotted in

TABLE 1. Experimental results at 0.1 MPa

Humidity buffer	Run no.	*T* (°C)*	Mass of Initial sample (mg)†	Duration (h)	Mass change (mg)
KNO_3					
	1	41.40	452.57	93	+1.65
	2	41.40	546.84	93	+2.92
	3	(42.18)	545.03	96	+3.15
	4	(42.18)	451.45	96	+0.25
	5	(42.38)	546.58	73	–0.29
	6	(42.38)	450.80	73	–0.12
	7	42.65	451.70	94	–0.90
	8	42.65	548.18	94	–1.60
	9	43.16	454.22	118	–2.77
	10	43.16	549.56	118	–4.53
KBr					
	1	(34.07)	466.99	120	+0.16
	2	(34.07)	562.40	120	+0.28
	3	(34.56)	561.22	96	–0.33
	4	(34.56)	465.61	96	–0.14
	5	35.14	562.68	119	–1.46
	6	35.14	467.15	119	–1.54
$NaNO_3$					
	1	(28.05)	562.70	65	+0.39
	2	(28.05)	467.10	65	+0.35
	3	(29.04)	563.09	95	–0.69
	4	(29.04)	467.45	95	–0.46
KI					
	1	17.01	438.09	95	+2.26
	2	17.01	382.82	95	+3.41
	3	17.97	379.61	65	+3.21
	4	17.97	435.60	65	+2.49
	5	20.16	440.35	120	+1.43
	6	20.16	386.23	120	+1.59
	7	21.19	441.78	119	+0.55
	8	21.19	387.82	119	+0.30
	9	(23.24)	442.17	72	+0.17
	10	(23.24)	387.94	72	+0.08
	11	24.04	388.12	96	+0.00
	12	24.04	442.33	96	–0.01
	13	(24.25)	442.34	96	–0.05
	14	(24.25)	388.02	96	-0.05
	15	25.06	388.06	95	–0.56
	16	25.06	442.29	95	–0.42
	17	25.90	437.26	73	–1.66
	18	25.90	381.34	73	-1.73
NaBr					
	1	8.81	415.67	68	+6.97
	2	8.81	420.71	68	+4.52
	3	14.06	419.15	96	+0.17
	4	14.06	416.20	96	+0.27
	5	14.06	442.18	96	+0.12
	6	(14.53)	441.87	93	+0.26
	7	(14.53)	387.50	93	+0.24
	8	(14.53)	415.20	93	+0.69
	9	(14.53)	418.93	93	+0.76
	10	(14.83)	417.13	46	-0.93
	11	(14.83)	419.95	46	-0.80
	12	(14.83)	442.50	46	–0.32
	13	15.42	387.70	42	–0.10
	14	15.43	422.41	52	–2.46
	15	15.43	442.84	52	–0.34
	16	16.17	437.59	73	–0.78
	17	16.17	441.63	73	–1.64
	18	17.01	438.88	95	–0.77
	19	17.01	435.64	95	–1.06
	20	17.97	439.99	65	–1.11
	21	17.97	436.81	65	–1.17

* Values in parentheses were used to bracket the reaction.
† Starting material consisted of a mixture of $CoSO_4 \cdot 7H_2O$ and $CoSO_4 \cdot 6H_2O$.

Figure 1. In Figure 1, the circles along each humidity-buffer curve represent reversal points, and the thick solid curve is the least-squares regression of these reversal points. Previous published results are also plotted for comparison.

Thermodynamic analysis

Equilibrium constants and ΔG_r° values for Reaction 1 were obtained from our experimental data using Equation 2 and these values are listed in Tables 2 and 3.

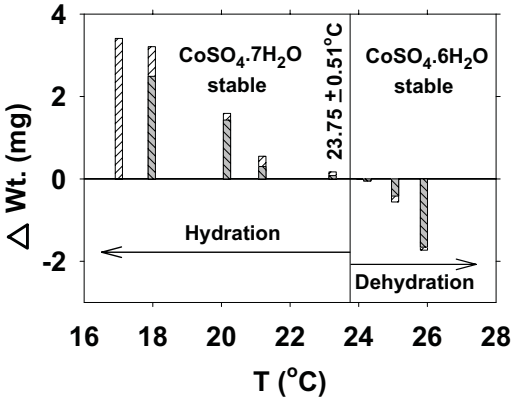

FIGURE 2. Experimental results showing weight changes of the bieberite-moorhouseite mixtures (381 to 442 mg) equilibrated with the KI-saturated buffer solution at fixed temperatures for 65 to 120 hours. Plotted are results listed in Table 1; two samples were run at each temperature and patterns indicate different samples. The equilibrium point was bracketed between 23.24 and 24.25 °C.

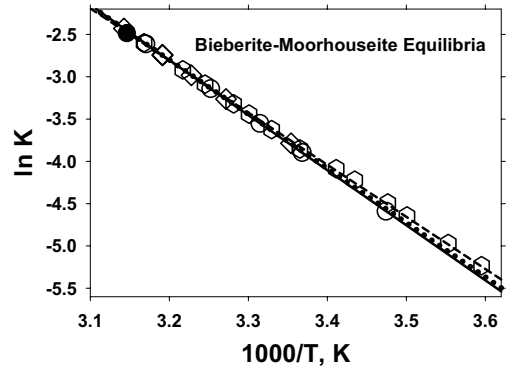

FIGURE 3. ln *K* vs. 1/*T* plot for the bieberite-moorhouseite equilibria at 0.1 MPa. Circles are current data from Table 2, and the solid line is a least-squares regression of the data. Data of Carpenter and Jette (1923) are shown by diamonds between 25 and 45.17 °C; the dotted line is a least-squares regression of the data. Data of Broers and Van Welie (1965) between 3 and 42.5 °C are shown by hexagons; the dashed line is a least-squares regression of the data. The large dot at the upper left corner is the invariant point at 44.7 °C for the assemblage bieberite + moorhouseite + aqueous solution + vapor (BMAV) reported by Broers and Van Welie (1965). For clarity, some previous data at 25 °C are not plotted. The regression lines based on the data of Wagman et al. (1982) and DeKock (1982) are very close to the solid line, and for clarity they are not shown.

Figure 3 shows the relation between ln *K* and 1/*T* for Reaction 1; our reversal data can be represented by $\ln K\ (\pm 0.013) = 18.03 - 6509.43/T$. The standard enthalpy of reaction, ΔH_r°, was calculated according to the relation:

$$\partial (\ln K)/\partial (1/T) = -\Delta H_r^\circ/R \quad (3)$$

The value of ΔH_r° for Reaction 1 is listed in Table 3, and the entropy of reaction, ΔS_r°, was calculated from the relation:

$$\Delta G_r^\circ = \Delta H_r^\circ - T\,\Delta S_r^\circ \quad (4)$$

and is also listed in Table 3. These derived thermodynamic data are compared with previous data in Table 3. Note that the uncertainties listed in Table 3 were derived from those associated with equilibrium temperatures and humidity buffers assuming

TABLE 2. Derived equilibrium constants for reaction 1 at 0.1 MPa

Humidity buffer	T (°C)†	$f^*_{H_2O}$ (MPa) ‡	% RH§	ln K
NaBr	14.68±0.15	0.0016714	60.78±0.05	–4.589±0.010
KI	23.75±0.51	0.0029414	69.12±0.11	–3.896±0.033
$NaNO_3$	28.55±0.50	0.0039061	73.47±0.11	–3.549±0.031
KBr	34.32±0.25	0.0054201	79.85±0.03	–3.140±0.014
KNO_3	42.28±0.10	0.0083289	88.15±0.04	–2.612±0.058

† Equilibrium T; mean of the two values used to bracket equilibrium (see Table 1). The uncertainty listed is half of the difference of the bracket values.
‡ Calculated from Haar et al. (1984).
§ Calculated from Greenspan (1977). Uncertainties are also based on Greenspan (1977).

TABLE 3. Derived thermodynamic data for Reaction 1 at 298.15K and 0.1 MPa

$\Delta G_r°$ (kJ/mol)	$\Delta H_r°$ (kJ/mol)	$\Delta S_r°$ [J/(mol·K)]	Reference
9.433 ± 0.008	54.12 ± 0.13	149.9 ± 0.5	This study
9.344	–	–	Wiedemann (1874)
9.450	–	–	Schumb (1923)
9.393	53.36	147.5	Carpenter and Jette (1923)
9.450	–	–	Diesnis (1935)
9.315	51.25	140.7	Broers and Van Welie (1965)
9.488	54.51	150.7	Wagman et al. (1982)
9.470	54.31	150.4	DeKock (1982)

no uncertainties for the vapor pressure of pure water.

As shown in Table 3 and Figures 1 and 3, our data are in excellent agreement with most of previous vapor-pressure measurements at and above 25 °C (Wiedemann 1874; Schumb 1923; Carpenter and Jette 1923; Diesnis 1935; Broers and Van Welie 1965). Our data for the bieberite-moorhouseite equilibria at lower temperatures are slightly lower in %RH than the values reported by Diesnis (1935) and Broers and Van Welie (1965), but are consistent with most of the high-temperature data, as demonstrated in Figures 1 and 3. Also, our data agree well with the thermodynamic data compiled by Wagman et al. (1982), and those compiled by DeKock (1982). Our value for $\Delta G_r°$ is 0.05 kJ/mol lower than the value reported by Wagman et al. (1982), and 0.04 kJ/mol lower than the value of DeKock (1982); these differences are well within the uncertainties of their estimates.

DISCUSSION

To verify our experimental results, we compared the invariant point for the assemblage bieberite + moorhouseite + aqueous solution + vapor (BMAV) derived from our results with that predicted by vapor-pressure measurements (Carpenter and Jette 1923; Broers and Van Welie 1965). The temperature of the invariant point for the assemblage BMAV is most likely near 44.7 °C (horizontal solid line in Fig. 1), as reported by Broers and Van Welie (1965); this temperature is between the values of 43.3 and 45.1 °C, reported by Rohmer (1939) and Carpenter and Jette (1923), respectively. Also shown in Figure 1 are the stability boundaries between bieberite and aqueous solution (Broers and Van Welie 1965) and between moorhouseite and aqueous solution (Carpenter and Jette 1923; Broers and Van Welie 1965). Extrapolation of the current bieberite-moorhouseite boundary to 44.7 °C yields 91.1% RH for the BMAV invariant point; this value agrees well with those reported by Carpenter and Jette (1923) and Broers and Van Welie (1965) at 91.4 and 89.9% RH (large open triangle at 44.7 °C shown in Fig. 1), respectively.

The results of the present study and those of Chou et al. (2002), Chou and Seal (2004), and Chou and Seal (2003a, 2003b) further confirm the conclusion of Hemingway et al. (2002) that the Gibbs free energy contribution for each water of crystallization in hydrated sulfate salts, except for the first water, is about –238.0 kJ/mol. The Gibbs free energy contribution for each water of crystallization can be calculated from the experimental results of this study for Reaction 1 by the equation:

$$\Delta G°_{xw,\,298.15K} = -(G°_{r,\,298.15K} - nG°_{f,\,H_2O,\,298.15K})/n \quad (5)$$

where $G°_{xw,\,298.15K}$ is the Gibbs free energy contribution for each additional water of crystallization at 298.15 K, $G°_{r,\,298K}$ is the Gibbs free energy of the reaction at 298.15 K, $G°_{f,\,H_2O,\,298.15K}$ is the Gibbs free energy of formation from elements for water at 298.15 K (Cox et al. 1989), and n is the stoichiometric coefficient for water in the dehydration reaction. For Reaction 1, $G°_{r,\,298.15K}$ is 9.433 kJ/mol, $G°_{f,\,H_2O,\,298.15K}$ is –228.6 kJ/mol (Cox et al. 1989), and n is 1, which yields a $G°_{xw,\,298.15K}$ of –238.03 kJ/mol. For melanterite-rozenite and chalcanthite-bonattite equilibria (Chou et al. 2002), calculated values for $G°_{xw,\,298K}$ are –238.34 and –239.90 kJ/mol, respectively. The value for the goslarite-bianchite equilibria is –238.23 kJ/mol (Chou and Seal 2005), for epsomite-hexahydrite equilibria is –238.73 kJ/mol (Chou and Seal 2003a), and for morenosite-retgersite equilibria is –237.44 kJ/mol (Chou and Seal 2003b).

The scarcity of the Co-sulfate minerals bieberite, moorehouseite, and aplowite is due, in part, to the scarcity of primary Co-sulfide minerals in nature. Common Co-sulfide minerals include linnaeite [Co_3S_4], carrollite [$Cu(Co, Ni)_2S_4$], cobaltite [CoAsS], and glaucodot [(Co, Fe)AsS]. These most commonly occur as accessory minerals in sulfide deposits primarily mined for Cu or Ni. The substitution of Co in pyrite and pyrrhotite is probably a more important precursor to Co-sulfate minerals. Experimental studies at 400 and 500 °C have demonstrated that the concentration of cobalt in pyrite is limited to less than 2 mol% CoS_2, whereas pyrrhotite shows complete solid solution with its Co counterpart (Wyszomirski 1980; Tauson and Akimov 1991). Nevertheless, the occurrence of Co-bearing sulfide minerals in nature is also limited by the low crustal abundance of Co (25 mg/kg; Craig et al. 1998). The scarcity can also be attributed to the fact that Co can readily substitute into other more-common simple sulfate minerals. The orthorhombic sulfates epsomite [$MgSO_4·7H_2O$], goslarite [$ZnSO_4·7H_2O$], and morenosite [$NiSO_4·7H_2O$] all can accept between 25 and 55 mol% Co (Jambor et al. 2000). Solid solution in the more common melanterite group, which is monoclinic and isostructural with bieberite, would be expected to be greater.

Reports of Co-sulfate minerals are not common. Bieberite is the most common, followed by moorhouseite and aplowite (Table 4). Invariably, all of the occurrences appear to be secondary alteration products of sulfide or arsenide minerals. Textural descriptions for all of the occurrences are insufficient to determine which minerals may be inferred to be in equilibrium. The presence of bieberite generally restricts the conditions at Leogang and the Rauris Valley (Austria), the Alfredo mine (Spain), the La Motte mine (USA), and Ticino (Switzerland) to humidities in excess of 60 percent assuming temperatures greater than 10 °C (Fig. 4). The presence of moorhouseite and aplowite at Walton (Canada) places this assemblage along the undetermined buffer curve corresponding to this assemblage, somewhere at lower humidities than the moorhouseite-bieberite curve. The mineral pairs from Saint Joachimsthal (Czech Republic) seem to record a range of disequilibrium humidities and temperatures,

TABLE 4. Selected mineralogy of cobalt-sulfate occurrences

Location	Cobalt sulfates	Other sulfates	Cobalt sulfides and arsenides	Other sulfides	Misc. minerals	References
Leogang, Austria	Bb			Py, Mc, Po	Lm, Gt, Er	Paar (1987)
Rauris Valley, Austria	Bb	Gyp		Py, Po	Lm, Gt	Schebesta (1984)
Walton, Nova Scotia, Canada	Mh, Ap			Py		Jambor and Boyle (1965)
St. Joachimsthal, Czech Republic	Bb, Mh	Mr, Rt, Nh, Rz, Me, Ha, Ma, Sz	Gl, Sk		Er	Hloušek and Tvrdý (2002)
Wildermann Mine, Germany	Bb	Ch, Rz, Sd, Rt, Mr	Sk, Sg	Py		Schnorrer et al. (2000)
Alfredo Mine, Rio Tinto, Spain	Bb	Me, Ch, Ma, Ha, Ep, Gy		Py		Garcia-Garcia (1992)
La Motte Mine, Missouri, U.S.A.	Bb					Kidwell (1946)
Ticino, Switzerland	Bb		Ln	Py	Ht, Lm	Schatz (1975)
Corinth Isthmus, Greece	Ap					Schnitzer (1976)

Notes: Abbreviations: Ap, aplowite [$CoSO_4$•$4H_2O$]; Bb, bieberite [$CoSO_4$•$7H_2O$]; Ch, chalcanthite [$CuSO_4$•$5H_2O$]; Ep, epsomite [$MgSO_4$•$7H_2O$]; Er, erythrite [$Co_3(AsO_4)_2$•$8H_2O$]; Gl, glaucodot [(Co,Fe)AsS]; Gt, goethite [$Fe^{3+}O(OH)$]; Gy, gypsum [$CaSO_4$•$2H_2O$]; Ha, halotrichite [$Fe^{2+}Al_2(SO_4)_4$•$22H_2O$]; Ht, heterogenite [$Co^{3+}O(OH)$]; Lm, limonite [$Fe^{3+}O(OH)$]; Ln, linnaeite [$Co^{2+}Co^{3+}{}_2S_4$]; Ma, mallardite [$MnSO_4$•$7H_2O$]; Mc, marcasite [FeS_2]; Me, melanterite [$FeSO_4$•$7H_2O$]; Mh, moorhouseite [$CoSO_4$•$6H_2O$]; Mr, morenosite [$NiSO_4$•$7H_2O$]; Nh, nickelhexahydrite [β-$NiSO_4$•$6H_2O$]; Py, pyrite [FeS_2]; Rt, retgersite [α-$NiSO_4$•$6H_2O$]; Rz, rozenite [$FeSO_4$•$4H_2O$]; Sd, siderotil [$FeSO_4$•$5H_2O$]; Sg, siegenite [$(Ni,Co)_3S_4$]; Sk, skutterudite ($CoAs_3$); Sz, szomolnokite [$FeSO_4$•H_2O].

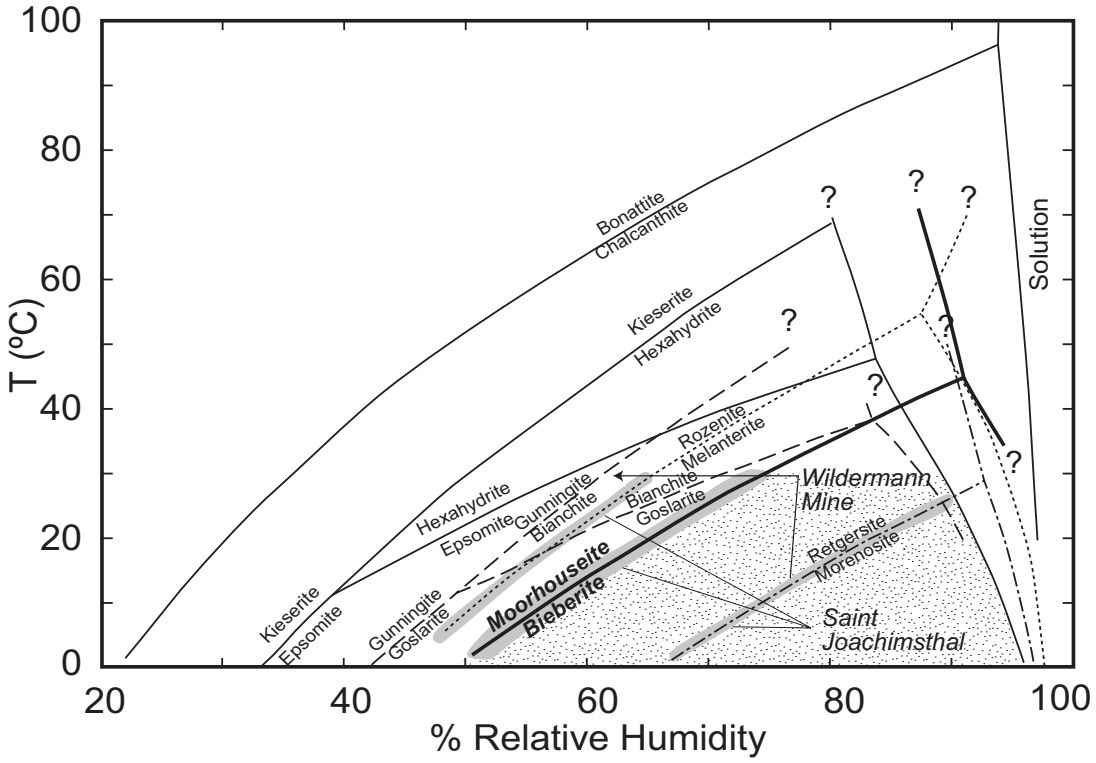

FIGURE 4. Hydrogenetic grid for selected hydrated metal-sulfate salts. Curves for bieberite and moorhouseite are from this study, those for melanterite and rozenite, and chalcanthite and bonattite are from Chou et al. (2002), those for goslarite, bianchite, and gunningite are from Chou and Seal (2005), those for epsomite, hexahydrite, and kieserite are from Chou and Seal (2003a), and those for morenosite and retgersite are from Chou and Seal (2003b). The stippled field indicates the stability of bierberite, the most common Co sulfate. The gray fields for various sites are derived from Table 4. Note the implied disequilibrium for St. Joachimsthal and the Wildermann mine. The arrow for the Wildermann mine indicates the approximate position for the siderotil-rozenite equilibrium position. For all sites, an annual temperature range from 0 to 30 °C was assumed.

although the effect of solid solutions is unknown (Hloušek and Tvrdý 2002). The lowest humidities or highest temperatures are recorded by the presence of rozenite and melanterite, followed in order of increasing humidity or decreasing temperature by moorhouseite and bieberite, and then by retgersite and morenosite (Fig. 4). At the Wildermann mine (Germany), the presence of retgersite and morenosite is consistent with the presence of bieberite as the only Co-sulfate mineral; however, the stability of siderotil with rozenite must lie at higher temperature or lower humidities than the moorhouseite-bieberite and the rozenite-melanterite curves (Fig. 4).

The addition of phase-equilibrium data for the system $CoSO_4$-H_2O improves the "hydrogenetic" grid that can be constructed for terrestrial ambient conditions by supplementing previous data (Fig. 4). The location of many of these dehydration reactions in the middle of the field of relative humidity and temperature conditions, and their rapid kinetics underscore the challenges of mineralogical characterization of samples as they relate to field conditions. The disequilibrium associations discussed above highlight the reality of these effects. The dissolution of these salts during summer storm events or spring-melt in snow-covered regions can significantly impact receiving watersheds. The

mineralogical controls on the partitioning of trace metals between dehydration products are poorly understood. Similarly, the role of differential partitioning of metals between sulfate salts and water in affecting surface runoff is inadequately known, although Alpers et al. (1994) demonstrated that preferential partitioning of Cu and Zn between melanterite and water can lead to seasonal variations in the Zn/Cu ratio of mine effluent at Iron Mountain, California. Ultimately, the greatest value from the present study may come from providing a sound thermodynamic basis from which to better understand solid-solution effects in multicomponent simple sulfate salts.

ACKNOWLEDGMENTS AND DISCLAIMER

We dedicate this paper to W.G. Ernst for his significant contributions in Earth sciences and education. We thank N.M. Piatak for X-ray analyses of our samples and J.M. Hammarstrom and B.S. Hemingway of U.S. Geological Survey for their critical review. We also thank J. Jambor for editorial review. The use of trade, product, industry, or firm names in this report is for descriptive purposes only and does not constitute endorsement by the U.S. Government.

REFERENCES CITED

Alpers, C.N., Nordstrom, D.K., and Thompson, J.M. (1994) Seasonal variations of Zn/Cu ratios in acid mine water from Iron Mountain, California. In C.N. Alpers and D.W. Blowes, Eds., Environmental geochemistry of sulfide oxidation. American Chemical Society Symposium Series, 550, 324–344.

Aslanian, S., Balarew, C., and Oikova, T. (1972) Isomorphic relations between $ZnSO_4 \cdot 7H_2O$ and $CoSO_4 \cdot 7H_2O$. Kristall und Technik, 7, 525–531 (in German).

Balarew, C., Karaivanova, V., and Aslanian, S. (1973) Isomorphic relations among the heptahydrate sulfates of single divalent metals (Mg, Zn, Ni, Fe, Co). Kristall und Technik, 8, 115–125 (in German).

Balarew, C. and Karaivanova, V. (1976) Isodimorphous cocrystallization in sulfate systems as a possibility of predicting the existence of crystal hydrates of the type $MSO_4.nH_2O$ ($M = Mn^{2+}, Fe^{2+}, Co^{2+}, Ni^{2+}, Cu^{2+}, Zn^{2+}, Cd^{2+}$). Zeitschrift für Anorganische und Allgemeine Chemie, 422, 283–288 (in German).

Broers, P.M.A. and Van Welie, G.S.A. (1965) The system $CoSO_4$-H_2O; vapour pressure measurements from 0° to 150°. Recueil des Travaux Chimiques des Pays-Bas et de la Belgique, 84, 789–798.

Carpenter, C.D. and Jette, E.R. (1923) The vapor pressures of certain hydrated metal sulfates. Journal of American Chemical Society, 45, 578–590.

Chou, I.M. and Seal, R.R., II (2003a) Determination of epsomite-hexahydrite equilibria by the humidity-buffer technique at 0.1 MPa with implications for phase equilibria in the system $MgSO_4$-H_2O. Astrobiology, 3, 619–630.

——— (2003b) Acquisition and evaluation of thermodynamic data for morenosite-retgersite equilibria at 0.1 MPa. American Mineralogist, 88, 1943–1948.

——— (2003c) Acquisition and evaluation of thermodynamic data for bieberite-moorhouseite equilibria at 0.1 MPa. GSA Abstracts with Programs, 34, 634.

——— (2005) Determination of goslarite-bianchite equilibria by the humidity-buffer technique at 0.1 MPa. Chemical Geology, 215, 517–524.

Chou, I.M., Seal, R.R., II, and Hemingway, B.S. (2002) Determination of melanterite-rozenite and chalcanthite-bonattite equilibria by humidity measurements at 0.1 MPa. American Mineralogist, 87, 108–114.

Craig, J.R., Vokes, F.M., and Solberg, T.N. (1998) Pyrite: physical and chemical textures. Mineralium Deposita, 34, 82–101.

Cox, J.D., Wagman, D.D., and Medvedev, V.A. (1989) CODATA key values for thermodynamics. Hemisphere, New York, 271 p.

DeKock, C.W. (1982) Thermodynamic properties of selected transition metal sulphates and their hydrates. U.S. Bureau of Mines Information Circular, 9810, 1–45.

Diesnis, M. (1935) Sur la détermination des états hygrométriques critiques. Bulletin de la Société Chimique de France, 5, No. 2, 1901–1907.

Garcia-Garcia, G. (1992) Los sulfatos del pozo Alfredo; Minas de Riotinto. Azogue (Madrid), 9, 18–25.

Goldberg, R.N., Riddell, R.G., Wingard, M.R., Hopkins, H.P., Wulff, C.A., and Hepler, L.G. (1966) Thermochemistry of cobalt sulfate and hydrates of cobalt and nickel sulfates. Thermodynamic properties of Co^{2+} (aq) and the cobalt oxidation potential. The Journal of Physical Chemistry, 70, 706–710.

Greenspan, L. (1977) Humidity fixed points of binary saturated aqueous solutions. Journal of Research of the National Bureau of Standards—A. Physics and Chemistry, B1A, 89–96.

Haar, L., Gallagher, J.S., and Kelly, G.S. (1984) NBS/NRC steam tables: Thermodynamic and transport properties and computer programs for vapor and liquid states of water in SI units. Hemisphere, Washington, DC, 320 p.

Hemingway, B.S., Seal, R.R., II, and Chou, I-M. (2002) Thermodynamic data for modeling acid mine drainage problems. I. Compilation and estimation of data for selected soluble iron-sulfate minerals. U.S. Geological Survey Open File Report 02–161.

Hloušek, J., and Tvrdý, J. (2002) Interessante sekundär-mineralien aus Jáchymov. Lapis, 27, No. 7/8, 44–66.

Jambor, J.L. and Boyle, R.W. (1965) Moorhouseite and aplowite, new minerals from Walton, Nova Scotia. Canadian Mineralogist, 8, 166–171.

Jambor, J.L., Nordstrom, D.K., and Alpers, C.N. (2000) Metal-sulfate salts from sulfide mineral oxidation. In C.N. Alpers, J.L. Jambor, and D.K. Nordstrom, Eds., Sulfate minerals: Crystallography, geochemistry, and environmental significance, 40, 305–350. Reviews in Mineralogy and Geochemistry, Mineralogical Society of America, Washington, D.C.

Kidwell, A.L. (1946) Minerals of the Fredericktown, Missouri, mining district. Rocks and Minerals, 21, 750–753.

Malinin, A.A., Drakin, S.I., and Ankudimov, A.G. (1977) Measurement of equilibrium vapour pressure in stepwise dehydration by using saturated reference solutions. Russian Journal of Physical Chemistry, No. 6. Translated from Zhurnal Fizichekoi Khimii, 51, 1557–1558.

——— (1979) Equilibrium dehydration pressures of salt crystal hydrates. Russian Journal of Physical Chemistry, 53, 755. Translated from Zhurnal Fizichekoi Khimii, 53, 1332–1333 (1979).

Paar, W.H. (1987) Erze und Gangart-mineralien von Leogang. Lapis, 12, no. 9, 11–32.

Peterson, R.C. (2002) The relationship between Cu content and distortion in the atomic structure of melanterite from the Richmond mine, Iron Mountain, California. Canadian Mineralogist, 41, 937–949.

Polyanskii, N.G., Gorbunov, G.V., and Polyanskaya, N.L. (1976) Methods of studying ion-exchange resins. Izdatelstvo Khimiya, Moscow.

Rohmer, R. (1939) A l'etude du sulfate de nickel et du sulfate de cobalt. Annales de Chemie, 11, 611–721.

Schatz, R.H. (1975) Die Erzmineralien des kobaltführenden Pegmatits bei Claro im Tessin/Schweiz. Aufschluss, 26, 439–440.

Schebesta, K. (1984) Seltene Mineralien aus den Goldschlacken im Rauriser Tal. Lapis, 9, No. 3, 9–21.

Schnitzer, W.A. (1976) Seltene Salzausblühungen (aplowit) auf neogenen Gesteinen des Isthmus von Korinth. Annales Geologiques des Pays Helleniques, 28, 349–351.

Schnorrer, G., Schneider, J., Pfeiffer, F., and Hiller, V. (2000) Die Minerale der Grube Wildermann bei Müsen im Siegerland-Erstnachweis eines primären, sowie zweier sekundärer Uran-Minerale im rheinischen Schiefergebirge. Aufschluss, 51, 71–123.

Schumb, W.C. (1923) The dissociation pressures of certain salt hydrates by the gas-current saturation method. Journal of the American Chemical Society, 45, 342–354.

Siebke, W., Spiering, H., and Meissner, E. (1983) Cooperative pseudo-Jahn-Teller effect of the $Fe(H_2O)_6^{2+}$ complexes in the sulfate heptahydrates. Physics Review B, 27, 2730–2739.

Tauson, V.L., and Akimov, V.V. (1991) Effect of crystallite size on solid state miscibility: applications to the pyrite-cattierite system. Geochimica et Cosmochimica Acta, 55, 2851–2859.

Wagman, D.D., Evans, W.H., Parker, V.B., Schumm, R.H., Halow, I., Bailey, S.M., Churney, K.L., and Nuttal, R.L. (1982) The NBS tables of chemical thermodynamic properties. Selected values for inorganic and C_1 and C_2 organic substances in SI units. Journal of Physical Chemistry Reference Data, Vol. 11, supplement no. 2, 392 p.

Wiedemann, E. (1874) Über die Dissociation der wasserhaltigen Salze. Journal für praktische chemie, 9, 338–356.

Wyszomirski, P. (1980) The pure dry Fe-Co-S system at 400 °C. Neues Jahrbach für Mineralogie Abhandlungen, 139, 131–132.

MANUSCRIPT RECEIVED APRIL 29, 2004
MANUSCRIPT ACCEPTED OCTOBER 5, 2004
MANUSCRIPT HANDLED BY SORENA SORENSEN